Cold Welding of Au Nanostructures at Room Temperature

XU Haiying[1,2], *NI Yuan*[1,3], *MIAO Changzong*[1], *KAN Caixia*[1*], *SHI Daning*[1]

1. College of Science, Nanjing University of Aeronautics and Astronautics, Nanjing 211106, P. R. China;
2. Department of Mathematics and Physics, Nanjing Institute of Technology, Nanjing 211167, P. R. China;
3. Department of Mathematics and Physics, Jinling Institute of Technology, Nanjing 211169, P. R. China

(Received 20 September 2020; revised 30 December 2020; accepted 3 June 2021)

Abstract: The common Au nanostructures (nanospheres, nanorods and nanosheets) were prepared by the seed growth method to explore the cold welding phenomenon of these non-single crystal nanostructures at room temperature. Systematic studies show that the concentration of surfactant cetyltrimethylammonium bromide(CTAB) and drying conditions are important factors to determine the evolution and final configuration of nanostructures during welding. The key factor of cold welding is the concentration of surfactant as low as 0.3 mm / L, and the welding should be carried out under the condition of slow evaporation and sufficient relaxation time, rather than rapid drying process. At the same time, the structural evolution during the welding process of gold rod head and tail is simulated by combining the electronic microscope characterization and density functional theory, which reveals that the stability of the welding nanostructure is better than that of the dispersed nanostructure. In the slow evaporation process of Au nanostructures with the same crystal structure, the low surfactant attached to the surface of the nanoparticles increases the attraction between the nanoparticles, which makes the nanoparticles close to each other adhere due to the interaction, and improves the physical properties of the intersection due to the diffusion, epitaxy and surface relaxation of the metal surface atoms. The results provide a research basis for the physical property analysis of nanostructures and the construction of defect devices.

Key words: cold welding; Au nanostructures; oriented-attachment; room temperature; density function theory

CLC number: TB383 **Document code:** A **Article ID:** 1005-1120(2021)03-0492-09

0 Introduction

In the past few years, extensive efforts have been devoted from self-assembly of metal nanostructures to multifunctional units due to the particular coupling effects of surface plasmon resonance (SPR)[1]. The coupling effect arises from the interaction between small-sized nanoparticles, which is sensitive to the spatial arrangement of nanoparticles, the interparticle distance and the particle number of assembly. Particularly, polymers and small organic ligands are often used as stabilizers to achieve the desired self-assembling structures[2-3], which prevents the aggregation fo the adjacent particles that adsorbed on the surface of the nanoparticles. It is worth to note that gold nanoparticles are easy to approach and coalescence under an electron beam, similar to the welding process[4-5], which has been developed as a fabrication technique involving the process from the fusion and cooling of metals to the construction of a strong joint, such as ion beam deposition[6-7], thermal or laser heating[8-9], ultrasonic irradiating[10], and high-energy electron beam bombardment[11-12]. However, the process usually requires critical temperature and reaction condition, thus it is difficult to control localized heating at the nanoscale. Cold welding of nanostructures (nanoparticles[13], nanorods[4], and nanowires[14-16]) at room temperature have been investigated since two gold thin films were joined together in the 1940s. The metal nanostructures with clean surface can rapidly form a neck with the adjacent particles even at small

*Corresponding author, E-mail address: cxkan@nuaa.edu.cn.

How to cite this article: XU Haiying, NI Yuan, MIAO Changzong, et al. Cold welding of Au nanostructures at room temperature[J]. Transactions of Nanjing University of Aeronautics and Astronautics, 2021, 38(3): 492-500.

http://dx.doi.org/10.16356/j.1005-1120.2021.03.013

thermal activation, leading to surfactant-stabilized gold nanoparticles[17-18] or nanorods[19-20] assembled to micrometric-length gold nanowires by selective self-organization and cold welding[21-25]. Cold welding at the nanoscale can be widely applied into optoelectronic devices due to its operability in ambient condition and spontaneous nature. In addition, the coupling effect, especially for the localized field enhancement induced by the interaction of SPR would be extinct, as confirmed by finite-difference time-domain simulation. The characteristic modes (such as dipole or multipole resonance) are dominated in the resonance modes of the product[26-28]. While, current research mainly focuses on the process from cold welding of ultrathin single-crystalline nanostructures to the formation of nanoaggregations. The welding mechanism of the twinned crystalline nanostructures need to be further demonstrated.

Herein, we study cold welding phenomena of twinned crystalline nanostructures including Au nanoparticles, nanorods and nanoplates at room temperature. Effects of the structural configurations, surfactant concentration and drying condition on the welding are explored. The surfactant concentration is an important factor, which directly determines the cold welding of nanostructures. Combined with the experimental observation and density function theory (DFT) simulation, the structural evolution during the welding process was studied. It also can be found that the stability of the welded nanostructures is better than that of separated nanostructures due to the rearrange of atoms for reducing the surface energy. Cold welding has been regarded as a promising nanofabrication technique in ambient condition.

1 Experiment

1.1 Materials

Sodium tetrahydridoborate ($NaBH_4$, 99%), hydrochloric acid (HCl, 37%), Tetrachloroaurate ($HAuCl_4 \cdot 4H_2O$, 99.9%) and ascorbic acid (AA, ≥99.7%) were obtained from Sinopharm Chemicals. Cetyltrimethylammonium bromide (CTAB, 99%) was obtained from Nanjing Robiot Co. Trisodium citrate ($Na_3C_6H_5O_7 \cdot 2H_2O$) was obtained from Chengdu Kelong Chemicals. Deionized water (18.25 MΩ) was used in the experiment. All reagents were used without further purification.

1.2 Preparation of Au nanostructures

Au nanostructures (nanoparticles, nanorods and nanoplates) were synthesized with a rapid seed-mediated method. Briefly, the seed solution was prepared by addition of ice-cold, freshly prepared $NaBH_4$ (0.15 mL, 0.01 mol/L) to an aqueous solution composed of trisodium citrate (0.25 mL, 0.01 mol/L) and $HAuCl_4$ (0.125 mL, 0.01 mol/L). Then solution was stirred in the oil bath at 45 ℃ for 15 min and aged for 2 h at room temperature for further preparation of Au nanostructures.

(1) Preparation of Au nanorods. An aqueous solution of CTAB (10 mL, 0.1 mol/L), $HAuCl_4$ (50 μL, 0.05 mol/L), and 50 μL of freshly prepared ascorbic acid (AA, 0.1 mol/L) solution was used as the growth solution. The growth solution became colorless when the freshly prepared AA (50 μL, 0.1 mol/L) solution was added. The colorless solution was added to the as-prepared seed solution (50 μL) stepwise in intervals of 30 s. The reaction system was kept at 20 ℃ for 30 min. And the twinned Au nanorods colloids were obtained. The preparation of twinned Au nanorods is different from that of single crystalline Au nanorods, in which Ag^+ were applied and pH was adjusted.

(2) Preparation of Au nanopaltes. The Au nanoplates were prepared through adding foreign iodide ions in the growth solution and modifying the experimental parameters. An aqueous solution composed of CTAB (10 mL, 0.1 mol/L), $HAuCl_4$ (50 μL, 0.05 mol/L), KI (45 μL, 0.01 mol/L), NaOH (50 μL, 0.1 mol/L) and freshly prepared AA (0.2 mL, 0.1 mol/L) was used as the growth solution. The growth solution became colorless when the freshly prepared AA solution was added. The colorless solution was added to the as-prepared seed solution stepwise in intervals of 30 s. The reaction system was kept at 30 ℃ for 20 min for the growth of Au nanoplates.

(3) Preparation of Au nanospheres. Au nano-

spheres will be dominated in the sample, when the concentration of the reactants in the growth solution are deviated from the equilibrium value of the above nanorods and nanoplates.

1.3 Cold welding

The prepared samples (Au nanoparticles, nanorods and nanoplates) were dropped on a carbon-coated copper grid. And the cold welding of twinned nanostructures were carried out by a natural slow-evaporation process distinguished from the normal fast-dry on the substrate at room temperature (25—30 ℃), which is very similar to the general treatment method. The main difference is that the cold welding occurs without necessary for a fast-drying evaporation, and directly derives from the formation mechanism of the natural slow-evaporation process.

The overall morphologies of the samples were observed by transmission electron microscopy (TEM) JEOL-100CX and high-resolution transmission electron microscope (HRTEM) JEOL—2011.

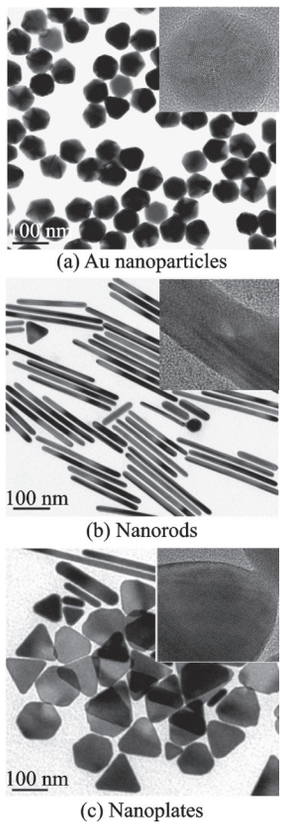

Fig.1 TEM images and the corresponding HRTEM images (inset)

2 Results and Discussion

Various of Au nanostructures, including nanoparticles, nanorods and nanoplates, were fabricated by seed-mediated method. Fig.1 shows the structural TEM images and corresponding HRTEM images (inset). It can be indicated that the nanoparticles (Fig.1(a)) and nanorods (Fig.1(b)) are five-twinned structures[29-30], and nanoplates is a crystalline structure with (111) basal plane (Fig.1(c)), accompanied with some single-twined crystalline induced from stacking-fault seeds[31].

Interestingly, the nanochain (or pair) composed of nanoparticles, nanorods, and nanoplate could be induced when the TEM samples were prepared by a natural slow-evaporation process different from the classical fast-evaporation method. Fig.2 show the TEM and HRTEM images of Au nanostructures under dry in the air. The assembled nanostructures are oriented-attachment with surrounding particles, and are welded together. Obviously, the nanoparticles with diameter of about 30 nm are analogous to nano-decahedron. According to the reported quantitative equilibrium phase map[32], it can be known that the decahedron over 15 nm is not a stable nanostructure. Therefore, large size of nano-decahedron would undergo Oswald ripening, to transfer into more stable nanostructures. For the touched Au decahedrons, outer atoms would move toward the neck, resulting in the formation of nanochain.

In order to further investigate the formation of welding, anisotropic Au nanostructures were processed with the similar method. From the TEM images of Fig.3(a) and Fig.3(b), it can be observed that Au nanorods are stable after three months at room temperature. However, when the concentration of surfactant CTAB is decreased, the welded Au nanorods can be formed. The critical concentration of surfactant bilayer CTAB is less than 0.3 mmol/L. When the concentration of CTAB is more than 0.5 mmol/L, no welding evolution during the assemble process can be observed, only several of configurations (such as end-to-end and L-shaped welding) can be formed, as shown in Fig.4(a), which is different from the conventional weld-

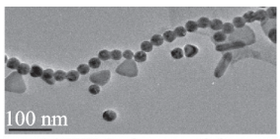

(a) TEM of anoparticles

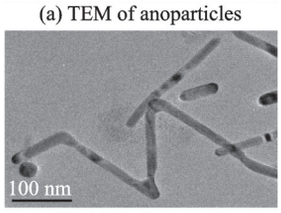

(b) TEM of nanorods

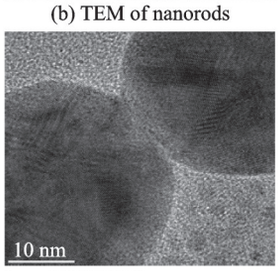

(c) Enlarged HRTEM between nanoparticles and nanorods

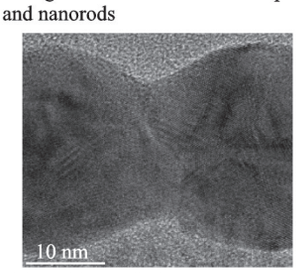

(d) Enlarged HRTEM between nanoparticles and nanoparticles

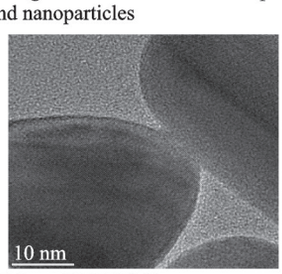

(e) Enlarged HRTEM between nanopaltes and nanorods

Fig.2 TEM images and the corresponding HRTEM images of Au nanochains composed of nanoparticles and nanorods

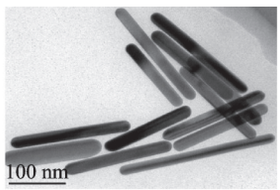

(a) Before three months at room temperature

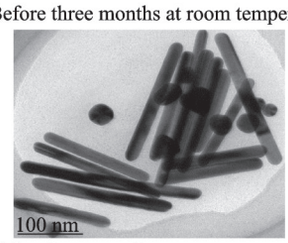

(b) After three months at room temperature

Fig.3 TEM images of Au nanorods colloids

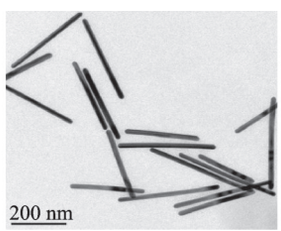

(a) 0.5 mmol/L

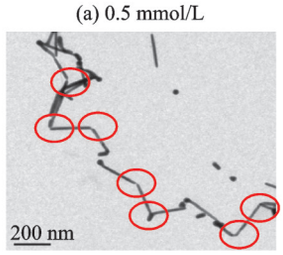

(b) 0.25 mmol/L for nanorods

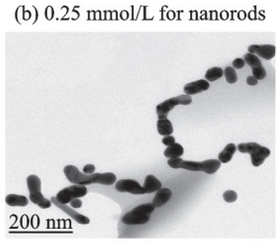

(c) 0.25 mmol/L for nanoparticles

Fig.4 TEM images of Au nanostructures with different concentration of CTAB

ing, since no mechanical force and external energy are exerted on the nanostructures surface. It is demonstrated by the formation of nanoparticle chains in the presence of CTAB (0.25 mmol), as shown in Fig.4(b). Additionally, nanochains or nanopairs composed of Au nanorods with different aspect ratios can be formed at low concentration of surfactant (0.25 mmol/L), as shown in Figs.5(a—c), illustrating the weld phenomenon is independent on the size of Au nanorods within the nanometer size range.

Fig.6 shows the junctional details between different Au nanoparticles. It can be found that these nanostructural junctions present different crystalline planes due to Au atoms redistribute along with the interface between nanoparticles. Different types of welding including end-to-end (Fig.6(a1)) or L-shape (Fig.6(b1)) for nanorods with intertwinning crystalline planes can be captured. Additionally, it can be observed that nanorods can be combined and welded with nanoparticles (Fig.6(c1)) and one-dimensional nanoplates (Fig.6(d1)). This illustrates that the evolution and final configuration of nano-

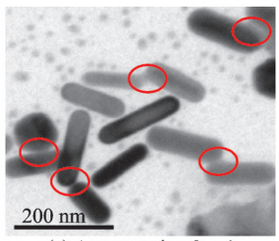

(a) Aspect ratio: 3—4

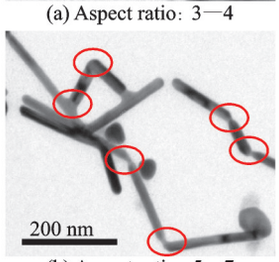

(b) Aspect ratio: 5—7

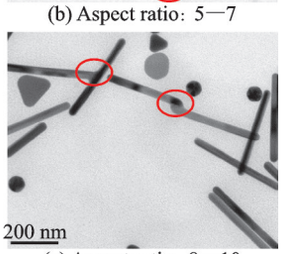

(c) Aspect ratio: 8—10

Fig.5 TEM images of Au nanorods with different aspect ratios in the presence of CTAB (0.25 mmol/L)

structures depend on the initial structure and state of the system, and cold welding is irrelevant to the initiation of the crystal indices.

Furthermore, from the corresponding HRTEM images in Figs.6(a2, b2, c2, d2), it can be demonstrated that all dislocations at this observed grain boundary have the shortest Burgers vector, which indicate that the welded nanochain experiences a stretching process, where a plastic deformation can be formed. Plastic deformation proceeds gradually with the emission of dislocation and annihilation of boundary, indicating that structural reorganization occurred at the cross-butting point of the nanoparticles, which can be attributed to the orientation and surface relaxation of the atoms in the nanoparticle.

In addition to the concentration of surfactant, the effect of evaporation condition on welding was also investigated. The nanoparticles colloids in the presence of CTAB (0.25 mmol/L) were dropped on the TEM substrates, following dried at room temperature (25—30 ℃) and heated oven, respec-

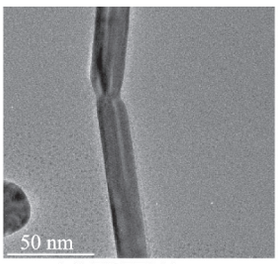

(a1) HRTEM image

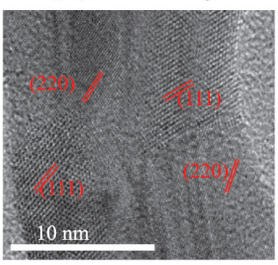

(a2) Partial enlarged HRTEM image
(a) Head-to-head between Au nanorods

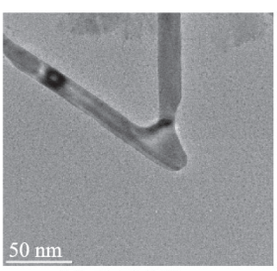

(b1) HRTEM image

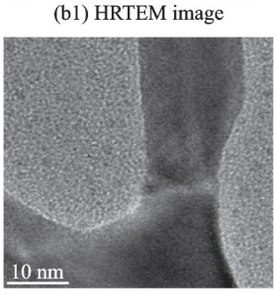

(b2) Partial enlarged HRTEM image
(b) L-shaped between Au nanorods

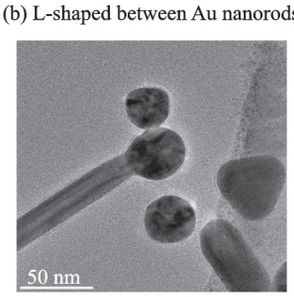

(c1) HRTEM image

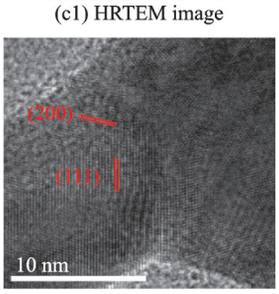

(c2) Partial enlarged HRTEM image
(c) Head-to-head between Au nanorods and nanoparticles

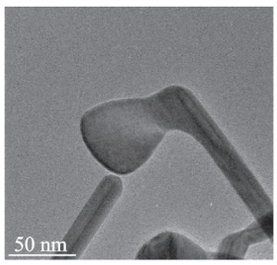

(d1) HRTEM image

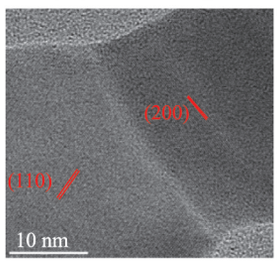

(d2) Partial enlarged HRTEM image
(d) L-shaped between Au nanorods and nanoplates

Fig.6 HRTEM images of welding junctions for different types of nanostructures

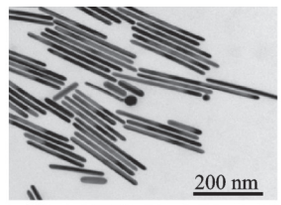

(a) In the air

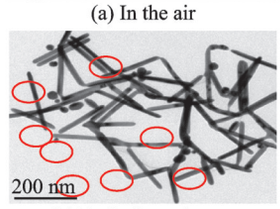

(b) In the heated oven

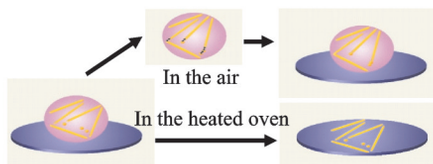

(c) Schematic illustration of different drying process

Fig.7 TEM images of dried Au nanostructures

tively. It can be found that the samples dried in the heated oven would quickly deposit and mono-dispersed on the substrate, as shown in Fig.7(a). While the nanoparticles would interact with adjacent particles during the process of natural slow-evaporation, as shown in Fig.7(b). Obviously, high temperature can promote the drying and depositing of the samples on the substrate, decreasing the interaction of the adjacent particles during the process of natural drying. Fig.7(c) shows the schematic illustration of different drying processes. The low concentration of surfactant and interaction of nanoparticles lead to the cold welding by particles attachment. The oriented-attachment is attributed to the strong Van der Waals force. In addition, the colloidal surfactant must be sufficiently weak to allow the nanoparticles to approach each other down a critical distance, where Van der Waals interactions within this distance can cause further attraction[19].

The diffusion barrier for a single metal atom on a clean surface of nanostructure is about 1.0 eV, which is enough for small thermal activation to trigger atomic diffusion[13,33]. Due to the high surface energy on the end surface of nanorods, the slightly oblique with a few internal defects of nanorods is formed before welding. A few dislocations nucleate and propagate on the (111) close packed plane (slip plane) on the surface of the nanorods. Thus, the two approaching nanorods are initially welded with an incomplete jointing area, and emerged to a single nanorod under the Van der Waals attractive force.

Based on the experimental results, DFT was also applied to explore the evolution of Au nanostructures and corresponding strain energy for the welding of head-to-head nanorods. The caculated structural evolution is consistent with the experimental observation, as shown in Fig.8. In the simulation, the initial distance between the two nanorods is set as 9 nm, and then the two nanorods approach slowly at a certain step size (450—650 steps with 0.02 nm/step) with a mechanical force. Fig.8(a) shows the structural evolution from the two approaching nanorods to the welded nanostructure under the mechanical force. An obvious atoms diffusion, oriented attachment and surface relaxation can be observed, as well as lattice recombination at the cross-point can be captured. This phenomenon is consistent with the experimental results shown in Fig.8(b). Meanwhile, the strain energy as a function of displacement in the cold welding of head-to-head nanorods is shown in Fig.8(c). In which, the abscissa describes the relative distance between the nanorods and initial position. Compared with monomer, the strain energy of welded nanostructures is

decreased, illustrating that the stability of welded nanorods is improved, which can be attributed to the minimized surface caused by rearrange of the atoms as the external force is transformed to the strain energy of the structure. Small-sized crystal with higher surface-to-volume ratio possesses much more high-energy adatoms, which tend to escape from the active sites to form thermodynamic stable crystal.

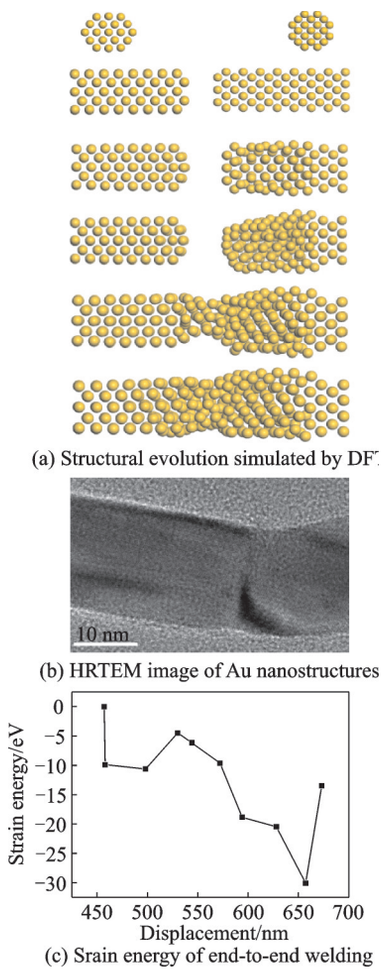

Fig.8 Structural evolution and property analysis for welding of end-to-end nanorods

3 Conclusions

In summary, various of Au nanostructures (Au nanoparticles, nanorods and nanoplates) were successfully synthesized, and cold welding phenomena of these non-single crystalline nanostructures without crystals melting were explored. Systematic studies reveal that the surfactant (CTAB) concentration and drying condition were important factors which determined the evolution and final configuration of nanostructures on the welding. The concentration of surfactant as low as 0.3 mmol/L is the critical element of cold welding, and welding occurs at slow evaporation with necessary for enough relaxation time as opposed to in-situation deposition for rapid drying. Combined with the experimental observations and DFT simulations, the structural evolution in the welding process is studied. It also can be found that the stability of the welded nanostructures is better than that of dispersed nanostructures due to the improved physical properties in the cross-point caused by the diffusion, epitaxy and surface relaxation of atoms. Cold welding may provide great opportunities in low-cost nanofabrication of nanodevice.

References

[1] PENG P, LIU L, GERLICH A P, et al. Self-oriented nanojoining of silver nanowires via surface selective activation[J]. Particle & Particle Systems Characterization, 2013, 30(5): 420-426.

[2] MARINO-LOPEZ A, BLANCO-FORMOSO M, FURINI L N, et al. Spontaneous formation of cold-welded plasmonic nanoassemblies with refracted shapes for intense raman scattering[J]. Langmuir, 2019, 35(11): 4110-4116.

[3] LIU J S, KAN C X, LI Y L, et al. End-to-end and side-by-side assemblies of gold nanorods induced by dithiol poly(ethylene glycol)[J]. Applied Physics Letters, 2014, 104(25): 1-6.

[4] DAI G L, WANG B J, XU S, et al. Side-to-side cold welding for controllable nanogap formation from "dumbbell" ultrathin gold nanorods[J]. ACS Applied Materials & Interfaces, 2016, 8(21): 13506-13511.

[5] LIM T H, MCCARTHY D, HENDY S C, et al. Real-time TEM and kinetic monte carlo studies of the coalescence of decahedral gold nanoparticles[J]. Acs Nano, 2009, 3(11): 3809-3813.

[6] MULDERS J J L. Purity and resistivity improvements for electron-beam-induced deposition of Pt[J]. Applied Physics A—Materials Science & Processing, 2014, 117(4): 1697-1704.

[7] AKANDE W O, CAO Y F, YAO N, et al. Adhesion and the cold welding of gold-silver thin films[J]. Journal of Applied Physics, 2010, 107(4): 1-4.

[8] NAM H, PARK C, KIM C, et al. Effect of post

weld heat treatment on weldability of high entropy alloy welds[J]. Science and Technology of Welding and Joining, 2018, 23(5): 420-427.

[9] ZAPICO E P, LUTEY A H A, ASCARI A, et al. An improved model for cold metal transfer welding of aluminium alloys[J]. Journal of Thermal Analysis and Calorimetry, 2018, 131(3): 3003-3009.

[10] YURIOKA N, HORII Y. Recent developments in repair welding technologies in Japan[J]. Science and Technology of Welding and Joining, 2006, 11(3): 255-264.

[11] HE L J, SU H H, XU J H, et al. Experimental investigation on the machinability of Ti_2AlNb intermetallic alloy[J]. Transactions of Nanjing University of Aeronautics and Astronautics, 2017, 34(5): 1-9.

[12] MARYA S, GERARD P. Welding and joining of titanium and its alloys. Trends and developments in France[J]. Rare Metal Materials and Engineering, 2006, 35: 15-20.

[13] WAGLE D V, BAKER G A. Cold welding: A phenomenon for spontaneous self-healing and shape genesis at the nanoscale[J]. Materials Horizons, 2015, 2(2): 157-167.

[14] PEREIRA Z S, DA SILVA E Z. Cold welding of gold and silver nanowires: A molecular dynamics study[J]. Journal of Physical Chemistry C, 2011, 115(46): 22870-22876.

[15] LU Y, HUANG J Y, WANG C, et al. Cold welding of ultrathin gold nanowires[J]. Nature nanotechnology, 2010, 5(3): 218-224.

[16] XU F, XU W, MAO B X, et al. Preparation and cold welding of silver nanowire based transparent electrodes with optical transmittances $>90\%$ and sheet resistances <10 ohm/sq[J]. Journal of Colloid and Interface Science, 2018, 512: 208-218.

[17] CASILLAS G, PONCE A, VELAZQUEZ-SALAZAR J J, et al. Direct observation of liquid-like behavior of a single Au grain boundary[J]. Nanoscale, 2013, 5(14): 6333-6337.

[18] MORENO-MORENO M, ARES P, MORENO C, et al. AFM manipulation of gold nanowires to build electrical circuits[J] Nano Letters, 2019, 19(8): 5459-5468.

[19] LAZA S C, SANSON N, SICARD-ROSELLI C, et al. Selective cold welding of colloidal gold nanorods[J]. Particle & Particle Systems Characterization, 2013, 30(7): 584-589.

[20] ZHU C, PENG H C, ZENG J, et al. Facile synthesis of gold wavy nanowires and investigation of their growth mechanism[J]. Journal of the American Chemical Society, 2012, 134(50): 20234-20237.

[21] LIU L, YOO S H, PARK S. Synthesis of vertically aligned hollow platinum nanotubes with single crystalline nanoflakes[J]. Chemistry of Materials, 2010, 22(8): 2681-2684.

[22] YOON S S, KHANG D Y. Room-temperature chemical welding and sintering of metallic nanostructures by capillary condensation[J]. Nano Letters, 2016, 16(6): 3550-3556.

[23] LEE P, LEE J, LEE H, et al. Highly stretchable and highly conductive metal electrode by very long metal nanowire percolation network[J]. Advanced Materials, 2012, 24(25): 3326-3332.

[24] JIN Y X, LI L, CHENG Y R, et al. Cohesively enhanced conductivity and adhesion of flexible silver nanowire networks by biocompatible polymer sol-gel transition[J]. Advanced Functional Materials, 2015, 25(10): 1581-1587.

[25] CHA S H, KANG S H, LEE Y J, et al. Fabrication of nanoribbons by dielectrophoresis assisted cold welding of gold nanoparticles on mica substrate[J]. Science Reports, 2019, 9(1): 1-8.

[26] NI Y, KAN C X, XU H Y, et al. Split resonance modes of a AuBRC plasmonic nanosystem caused by the coupling effect[J]. Journal of Physics D—Applied Physics, 2016, 49(50): 505153.

[27] XU H Y, KAN C X, MIAO C Z, et al. Synthesis of high-purity silver nanorods with tunable plasmonic properties and sensor behavior[J]. Photonics Research, 2017, 5(1): 27-32.

[28] XU W, KAN C X, NI Y, et al. Controllable synthesis of Ag nanocubes via a polyol method[J]. Transactions of Nanjing University of Aeronautics and Astronautics, 2017, 34(4): 388-392.

[29] JOHNSON C J, DUJARDIN E, DAVIS S A, et al. Growth and form of gold nanorods prepared by seed-mediated, surfactant-directed synthesis[J]. Journal of Materials Chemistry, 2002, 12(6): 1765-1770.

[30] LI H C, KAN C X, YI Z G, et al. Synthesis of one dimensional gold nanostructures[J]. Journal of Nanomaterials, 2010: 1-8.

[31] KAN C X, WANG C S, LI H C, et al. Gold microplates with well-defined shapes[J]. Small, 2010, 6(16): 1768-1775.

[32] BARNARD A S, YOUNG N P, KIRKLAND A I, et al. Nanogold: A quantitative phase map[J]. ACS Nano, 2009, 3(6): 1431-1436.

[33] WU C D, FANG T H, WU C C. Size effect on cold-

welding of gold nanowires investigated using molecular dynamics simulations[J]. Applied Physics A—Materials Science & Processing, 2016, 122(3): 1-6.

Acknowledgements This work was supported by the National Natural Science Foundations of China (Nos. 11774171, 11874220, 21805137), the Open Funds of Key Laboratory for Intelligent Nano Materials and Devices of the Ministry of Education (Nos. INMD-2019M02, INMD-2020M03), the Scientific Foundation of Nanjing Institute of Technology (No.CKJB201708), and the Fundamental Research Funds for the Central Universities (No.NS2017047) provided by Nanjing University of Aeronautics and Astronautics.

Authors Dr. **XU Haiying** received his M. S. degree in physics from Southeast University, Nanjing, China, in 2005, and Ph.D. degree in College of Science, Nanjing University of Aeronautics and Astronautics (NUAA), Nanjing, China in 2017. Since July 2018, she has been a postdoctoral fellow in College of Science, NUAA. Her research interests include nanomaterial, and low-dimensional functional materials and devices.

Prof. **KAN Caixia** received her Ph.D. degree in condensed matter physics from Institute of Solid State Physics, Chinese Academy of Sciences in June 2004. From September 2004 to September 2006, she conducted Physics post-doctoral mobile station of Nanjing University. From September 2002 to November 2002, she conducted scientific research cooperation at the Max Planck Society Institute of Microstructure Physics in Germany. From November 2006, she engaged in teaching and scientific in College of Science, NUAA. In May 2007, she was promoted to associate professor at College of Science, and in May 2009, she was promoted to a full professor by exception at College of Science, NUAA. Her research interests include nanomaterial, low-dimensional functional materials and devices, and optical engineering.

Author contributions Dr. **XU Haiying** conducted the experiment, analysis and interpreted the results and wrote the manuscript. Dr. **NI Yuan** conducted the experimental operation, theoretical simulation, and wrote the manuscript. Dr. **MIAO Changzong** conducted the sample test and the discussion and background of the study. Prof. **KAN Caixia** designed the study, revised the manuscript and the results of theoretical simulation. Prof. **SHI Daning** conducted the background of the study and designed the study. All authors commented on the manuscript draft and approved the submission.

Competing interests The authors declare no competing interests.

(Production Editor: SUN Jing)

Au纳米结构的常温冷焊接研究

徐海英[1,2], 倪 媛[1,3], 缪长宗[1], 阚彩侠[1], 施大宁[1]

(1.南京航空航天大学理学院,南京 211106,中国; 2.南京工程学院数理部,南京 211167,中国;
3.金陵科技学院数理部,南京 211169,中国)

摘要:基于种子生长法制备了常见的Au纳米结构(纳米球,纳米棒和纳米片),并探究了这些非单晶纳米结构在常温下的冷焊接现象。系统研究表明,表面活性剂(Cetyltrimethylammonium bromide, CTAB)的浓度和干燥条件是决定焊接过程中纳米结构演变和最终构型的重要因素。表面活性剂浓度低至0.3 mmol/L是冷焊的关键因素,且焊接需在缓慢蒸发和足够的驰豫时间条件下进行,而非快速干燥过程。同时,结合电镜表征和密度泛函理论,模拟金棒头尾焊接过程中的结构演变,揭示焊接纳米结构的稳定性优于分散纳米结构:相同晶体结构的Au纳米结构在慢蒸发过程中,附着在纳米粒子表面的低表面活性剂增加了纳米粒子之间的吸引力,使得相互靠近的纳米粒子由于相互作用而出现附着,由于金属表面原子的扩散、外延和表面弛豫引起的交叉点物理性能的改善。本文结果为纳米结构的物性分析和缺陷器件的构建提供了研究基础。

关键词:冷焊接;金纳米结构;定向附着;常温;密度泛函理论